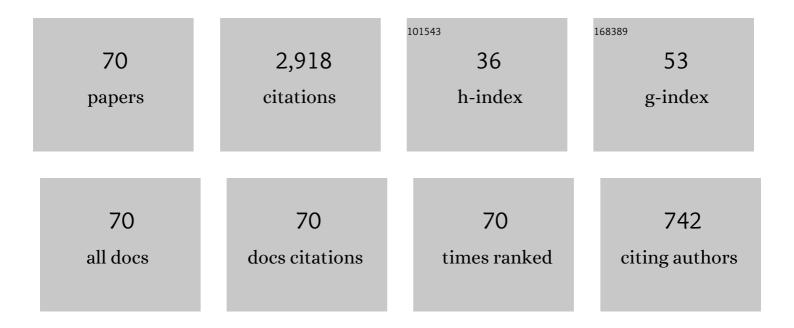
## Hongpeng Wu

List of Publications by Year in descending order

Source: https://exaly.com/author-pdf/11803675/publications.pdf Version: 2024-02-01



HONCRENC WU

#	Article	IF	CITATIONS
1	Beat frequency quartz-enhanced photoacoustic spectroscopy for fast and calibration-free continuous trace-gas monitoring. Nature Communications, 2017, 8, 15331.	12.8	213
2	Compact TDLAS based sensor design using interband cascade lasers for mid-IR trace gas sensing. Optics Express, 2016, 24, A528.	3.4	150
3	Quartz enhanced photoacoustic H2S gas sensor based on a fiber-amplifier source and a custom tuning fork with large prong spacing. Applied Physics Letters, 2015, 107, .	3.3	128
4	Atmospheric CH4 measurement near a landfill using an ICL-based QEPAS sensor with V-T relaxation self-calibration. Sensors and Actuators B: Chemical, 2019, 297, 126753.	7.8	127
5	Enhanced near-infrared QEPAS sensor for sub-ppm level H2S detection by means of a fiber amplified 1582 nm DFB laser. Sensors and Actuators B: Chemical, 2015, 221, 666-672.	7.8	91
6	Sub-ppb nitrogen dioxide detection with a large linear dynamic range by use of a differential photoacoustic cell and a 3.5 W blue multimode diode laser. Sensors and Actuators B: Chemical, 2017, 247, 329-335.	7.8	90
7	Single-tube on-beam quartz-enhanced photoacoustic spectroscopy. Optics Letters, 2016, 41, 978.	3.3	88
8	ppb-Level SO <sub>2</sub> Photoacoustic Sensors with a Suppressed Absorption–Desorption Effect by Using a 7.41 μm External-Cavity Quantum Cascade Laser. ACS Sensors, 2020, 5, 549-556.	7.8	79
9	Quartz-enhanced photoacoustic spectroscopy for multi-gas detection: A review. Analytica Chimica Acta, 2022, 1202, 338894.	5.4	79
10	High and flat spectral responsivity of quartz tuning fork used as infrared photodetector in tunable diode laser spectroscopy. Applied Physics Reviews, 2021, 8, .	11.3	76
11	Ppb-level QEPAS NO2 sensor by use of electrical modulation cancellation method with a high power blue LED. Sensors and Actuators B: Chemical, 2015, 208, 173-179.	7.8	70
12	Ppb-Level Quartz-Enhanced Photoacoustic Detection of Carbon Monoxide Exploiting a Surface Grooved Tuning Fork. Analytical Chemistry, 2019, 91, 5834-5840.	6.5	67
13	Three-Dimensional Printed Miniature Fiber-Coupled Multipass Cells with Dense Spot Patterns for ppb-Level Methane Detection Using a Near-IR Diode Laser. Analytical Chemistry, 2020, 92, 13034-13041.	6.5	67
14	Simultaneous dual-gas QEPAS detection based on a fundamental and overtone combined vibration of quartz tuning fork. Applied Physics Letters, 2017, 110, .	3.3	64
15	Compact photoacoustic module for methane detection incorporating interband cascade light emitting device. Optics Express, 2017, 25, 16761.	3.4	63
16	Ppb-level photoacoustic sensor system for saturation-free CO detection of SF6 decomposition by use of a 10 W fiber-amplified near-infrared diode laser. Sensors and Actuators B: Chemical, 2019, 282, 567-573.	7.8	63
17	Double acoustic microresonator quartz-enhanced photoacoustic spectroscopy. Optics Letters, 2014, 39, 2479.	3.3	58
18	Ppb-level gas detection using on-beam quartz-enhanced photoacoustic spectroscopy based on a 28ÂkHz tuning fork. Photoacoustics, 2022, 25, 100321.	7.8	57

Hongpeng Wu

#	Article	IF	CITATIONS
19	Dual-Gas Quartz-Enhanced Photoacoustic Sensor for Simultaneous Detection of Methane/Nitrous Oxide and Water Vapor. Analytical Chemistry, 2019, 91, 12866-12873.	6.5	53
20	Highly sensitive and selective CO sensor using a 233 μm diode laser and wavelength modulation spectroscopy. Optics Express, 2018, 26, 24318.	3.4	52
21	Light-induced thermo-elastic effect in quartz tuning forks exploited as a photodetector in gas absorption spectroscopy. Optics Express, 2020, 28, 19074.	3.4	51
22	Impact of Humidity on Quartz-Enhanced Photoacoustic Spectroscopy Based CO Detection Using a Near-IR Telecommunication Diode Laser. Sensors, 2016, 16, 162.	3.8	49
23	Highly sensitive SO_2 photoacoustic sensor for SF_6 decomposition detection using a compact mW-level diode-pumped solid-state laser emitting at 303 nm. Optics Express, 2017, 25, 32581.	3.4	49
24	Highly sensitive photoacoustic multicomponent gas sensor for SF <sub>6</sub> decomposition online monitoring. Optics Express, 2019, 27, A224.	3.4	49
25	Ppb-level H2S detection for SF6 decomposition based on a fiber-amplified telecommunication diode laser and a background-gas-induced high- <i>Q</i> photoacoustic cell. Applied Physics Letters, 2017, 111,	3.3	48
26	Broadband detection of methane and nitrous oxide using a distributed-feedback quantum cascade laser array and quartz-enhanced photoacoustic sensing. Photoacoustics, 2020, 17, 100159.	7.8	47
27	Quartz-enhanced photoacoustic sensor for ethylene detection implementing optimized custom tuning fork-based spectrophone. Optics Express, 2019, 27, 4271.	3.4	46
28	Quartz-enhanced photoacoustic spectroscopy for hydrocarbon trace gas detection and petroleum exploration. Fuel, 2020, 277, 118118.	6.4	43
29	Quartz-enhanced photoacoustic spectroscopy exploiting low-frequency tuning forks as a tool to measure the vibrational relaxation rate in gas species. Photoacoustics, 2021, 21, 100227.	7.8	43
30	Partial Least-Squares Regression as a Tool to Retrieve Gas Concentrations in Mixtures Detected Using Quartz-Enhanced Photoacoustic Spectroscopy. Analytical Chemistry, 2020, 92, 11035-11043.	6.5	42
31	Mid-Infrared Quartz-Enhanced Photoacoustic Sensor for ppb-Level CO Detection in a SF <sub>6</sub> Gas Matrix Exploiting a T-Grooved Quartz Tuning Fork. Analytical Chemistry, 2020, 92, 13922-13929.	6.5	42
32	Calculation model of dense spot pattern multi-pass cells based on a spherical mirror aberration. Optics Letters, 2019, 44, 1108.	3.3	42
33	High-concentration methane and ethane QEPAS detection employing partial least squares regression to filter out energy relaxation dependence on gas matrix composition. Photoacoustics, 2022, 26, 100349.	7.8	41
34	Fiber-Amplifier-Enhanced QEPAS Sensor for Simultaneous Trace Gas Detection of NH3 and H2S. Sensors, 2015, 15, 26743-26755.	3.8	38
35	Calibration-free mid-infrared exhaled breath sensor based on BF-QEPAS for real-time ammonia measurements at ppb level. Sensors and Actuators B: Chemical, 2022, 358, 131510.	7.8	38
36	H2S quartz-enhanced photoacoustic spectroscopy sensor employing a liquid-nitrogen-cooled THz quantum cascade laser operating in pulsed mode. Photoacoustics, 2021, 21, 100219.	7.8	37

HONGPENG WU

#	Article	IF	CITATIONS
37	Position effects of acoustic micro-resonator in quartz enhanced photoacoustic spectroscopy. Sensors and Actuators B: Chemical, 2015, 206, 364-370.	7.8	36
38	Compact and Highly Sensitive NO2 Photoacoustic Sensor for Environmental Monitoring. Molecules, 2020, 25, 1201.	3.8	34
39	Double antinode excited quartz-enhanced photoacoustic spectrophone. Applied Physics Letters, 2017, 110, .	3.3	33
40	Palm-sized methane TDLAS sensor based on a mini-multi-pass cell and a quartz tuning fork as a thermal detector. Optics Express, 2021, 29, 12357.	3.4	33
41	Compact QEPAS humidity sensor in SF6 buffer gas for high-voltage gas power systems. Photoacoustics, 2022, 25, 100319.	7.8	33
42	Application of acoustic micro-resonators in quartz-enhanced photoacoustic spectroscopy for trace gas analysis. Chemical Physics Letters, 2018, 691, 462-472.	2.6	30
43	Ppb-level nitric oxide photoacoustic sensor based on a mid-IR quantum cascade laser operating at 52 °C. Sensors and Actuators B: Chemical, 2019, 290, 426-433.	7.8	30
44	Scattered light modulation cancellation method for sub-ppb-level NO_2 detection in a LD-excited QEPAS system. Optics Express, 2016, 24, A752.	3.4	28
45	Acoustic Coupling between Resonator Tubes in Quartz-Enhanced Photoacoustic Spectrophones Employing a Large Prong Spacing Tuning Fork. Sensors, 2019, 19, 4109.	3.8	26
46	Quartz-enhanced photoacoustic NH3 sensor exploiting a large-prong-spacing quartz tuning fork and an optical fiber amplifier for biomedical applications. Photoacoustics, 2022, 26, 100363.	7.8	25
47	Generalized optical design of two-spherical-mirror multi-pass cells with dense multi-circle spot patterns. Applied Physics Letters, 2020, 116, .	3.3	20
48	Compact quartz-enhanced photoacoustic sensor for ppb-level ambient NO2 detection by use of a high-power laser diode and a grooved tuning fork. Photoacoustics, 2022, 25, 100325.	7.8	20
49	Dual quantum cascade laser-based sensor for simultaneous NO and NO2 detection using a wavelength modulation-division multiplexing technique. Applied Physics B: Lasers and Optics, 2017, 123, 1.	2.2	19
50	Multiple-sound-source-excitation quartz-enhanced photoacoustic spectroscopy based on a single-line spot pattern multi-pass cell. Applied Physics Letters, 2021, 118, .	3.3	16
51	Cavity-enhanced photoacoustic sensor based on a whispering-gallery-mode diode laser. Atmospheric Measurement Techniques, 2019, 12, 1905-1911.	3.1	15
52	Piezo-enhanced acoustic detection module for mid-infrared trace gas sensing using a grooved quartz tuning fork. Optics Express, 2019, 27, 35267.	3.4	12
53	Multi-Quartz Enhanced Photoacoustic Spectroscopy with Different Acoustic Microresonator Configurations. Journal of Spectroscopy, 2015, 2015, 1-6.	1.3	11
54	Acoustic Detection Module Design of a Quartz-Enhanced Photoacoustic Sensor. Sensors, 2019, 19, 1093.	3.8	10

Hongpeng Wu

#	Article	IF	CITATIONS
55	Simultaneous multi-gas detection between 3 and 4 μm based on a 2.5-m multipass cell and a tunable Fabry-Pérot filter detector. Spectrochimica Acta - Part A: Molecular and Biomolecular Spectroscopy, 2019, 216, 154-160.	3.9	9
56	Elliptical-tube off-beam quartz-enhanced photoacoustic spectroscopy. Applied Physics Letters, 2022, 120, .	3.3	9
57	Quartz-enhanced conductance spectroscopy for nanomechanical analysis of polymer wire. Applied Physics Letters, 2015, 107, 221903.	3.3	8
58	Near-Infrared Quartz-Enhanced Photoacoustic Sensor for H2S Detection in Biogas. Applied Sciences (Switzerland), 2019, 9, 5347.	2.5	7
59	Optical Detection Technique Using Quartz-Enhanced Photoacoustic Spectrum. International Journal of Thermophysics, 2015, 36, 1297-1304.	2.1	5
60	Quartz Enhanced Conductance Spectroscopy for Polymer Nano-Mechanical Thermal Analysis. Applied Sciences (Switzerland), 2020, 10, 4954.	2.5	3
61	Quartz Enhanced Photoacoustic Detection Based on an Elliptical Laser Beam. Applied Sciences (Switzerland), 2020, 10, 1197.	2.5	3
62	New Developments in Quartz-Enhanced Photoacoustic Sensing Real-World Applications. , 2020, , .		2
63	Design and Optimization of QTF Chopper for Quartz-Enhanced Photoacoustic Spectroscopy. International Journal of Thermophysics, 2015, 36, 1289-1296.	2.1	1
64	Single-tube on beam quartz-enhanced photoacoustic spectrophones exploiting a custom quartz tuning fork operating in the overtone mode. Proceedings of SPIE, 2017, , .	0.8	0
65	Near-infrared Quartz Enhanced Photoacoustic Sensor for Sub-ppm Level H2S Detection based on a Fiber-amplifier Source. , 2016, , .		0
66	Micro-resonator Parameter Optimization of a QEPAS Spectrophone using a Custom Quartz Tuning Fork with large Prong Spacing. , 2016, , .		0
67	Nitrogen Dioxide Detection by use of Photoacoustic Spectroscopy with a High Power Violet-Blue Diode Laser. , 2017, , .		0
68	Photoacoustic H2S Gas Sensor for SF6 Decomposition Analysis in an Electric Power System. , 2018, , .		0
69	Fast and calibration-free trace-gas monitoring based on beat frequency quartz-enhanced photoacoustic spectroscopy. , 2018, , .		0
70	Quartz-Enhanced Photoacoustic and Photothermal Spectroscopy. Applied Sciences (Switzerland), 2022, 12, 2613.	2.5	0